# Dynamics of electrons in quantum Hall bubble phases

R. Côté,[1] C. B. Doiron,[1] J. Bourassa,[1] and H. A. Fertig[2]
[1]*Département de Physique, Université de Sherbrooke, Sherbrooke, Québec, Canada, J1K 2R1*
[2]*Department of Physics and Astronomy, University of Kentucky, Lexington, Kentucky 40506-0055, USA*
(Received 16 April 2003; revised manuscript received 24 July 2003; published 27 October 2003)

In Landau levels $N>1$, the ground state of the two-dimensional electron gas (2DEG) in a perpendicular magnetic field evolves from a Wigner crystal for small filling $\nu^*$ of the partially filled Landau level, into a succession of bubble states with increasing number of guiding centers per bubble as $\nu^*$ increases, to a modulated stripe state near $\nu^*=0.5$. In this work, we show that these first-order phase transitions between the bubble states lead to measurable discontinuities in several physical quantities such as the density of states and the magnetization of the 2DEG. We discuss in detail the behavior of the collective excitations of the bubble states and show that their spectra have higher-energy modes besides the pinned phonon mode. The frequencies of these modes, at small wave vector **k**, have a discontinuous evolution as a function of filling factor that should be measurable in, for example, microwave absorption experiments.

DOI: 10.1103/PhysRevB.68.155327 PACS number(s): 73.43.−f, 73.20.Qt, 73.21.−b

## I. INTRODUCTION

It is now well established both theoretically[1] and experimentally,[2,3] that the two-dimensional electron gas (2DEG) ground state near half filling in the higher Landau levels ($N>1$) is the quantum Hall stripe state. Transport experiments have shown that this stripe state has an highly anisotropic longitudinal conductivity, i.e., $\sigma_{yy}\gg\sigma_{xx}$ (where $\hat{x}$ is the direction perpendicular to the stripes) and a Hall conductivity $\sigma_{xy}$ that is not quantized. Away from half filling, more precisely at *partial* filling factors around $\nu^*\approx 1/4$ and $\nu^*\approx 3/4$ in Landau level $N=2$, the isotropy of the longitudinal conductivity is restored and a minima appears in the diagonal resistance. Concomitantly, the Hall conductivity is quantized, but at a value equal to that of the nearest integer quantum Hall effect plateaus. These other ground states around $\nu^*\approx\frac{1}{4}$ and $\nu^*\approx\frac{3}{4}$ in $N=2$ have been called reentrant integer quantum Hall states (RIQHS).[4] Studies by Koulakov, Fogler, and Shklovskii and by Moessner and Chalker[1] suggest that the RIQHS are due to the formation of bubble states. These states can be described as triangular Wigner crystals of electron clusters. Each cluster (or ''bubble'') contains a fixed number $M$ of electrons such that, within them, the local filling factor is equal to one. The bubble states, being pinned by disorder, should be insulating in contrast to the stripe states. A review of these novel ground states in higher Landau level is given in Ref. 5.

The ground state of the 2DEG changes discontinuously as the partial filling factor $\nu^*$ is changed. In the Hartree-Fock approximation (HFA), the ground state is a Wigner crystal at small filling $\nu^*$ or, equivalently, a bubble state with one guiding center per bubble. As the partial filling is increased, bubble states with increasing number $M$ of electrons per bubble are stabilized so that the 2DEG evolves from the Wigner crystal, through a succession of bubble states, into finally the stripe state near half-filling. In Landau level $N$, it can be shown that (in the HFA) the last bubble state has $M=N+1$. The optimal number of guiding centers in a bubble is well approximated by the formula $M=3\nu^*N$ corresponding to an average separation between the bubbles equal to $a=3.3R_c$ where $R_c=\sqrt{2N+1}\ell$ is the cyclotron radius and $\ell=\sqrt{\hbar c/eB}$ is the magnetic length. This sequence of phase transitions in higher Landau levels has been verified by a number of authors. By comparing the energy of the Laughlin liquid at $\nu^*=\frac{1}{3}$ and $\nu^*=\frac{1}{5}$ with that of the bubble states in several Landau levels, Fogler and Koulakov[6] showed, within the HFA, that the bubble states are lower in energy than the Laughlin liquid at filling factor $\nu^*=\frac{1}{3}$ for $N\geqslant 2$ and at filling factor $\nu^*=\frac{1}{5}$ for $N\geqslant 3$. Rezayi *et al.*[7] used exact diagonalization studies on finite size systems to show the absence of fractional quantum Hall states (FHQS) in higher Landau levels and a tendancy to charge density wave (CDW) ordering. Recent calculations by Yoshioka and Shibata[8] using the density matrix renormalization group method (DMRG) basically confirm the Hartree-Fock scenario with some minor corrections. For $N=2$ and $N=3$, the DMRG gives a wider region of stability for the stripe phase than in the HFA. As a result, the last bubble state (that with $M=N+1$) is absent from the phase diagram. The transitions between different bubble states occur at slightly different filling factors in the two approaches. Both calculations, however, give first-order phase transitions between the bubble states and between the bubble and stripe states. The possibility of a continuous phase transition involving the deformation of the bubbles from a isotropic shape to a more elliptical shape as the stripe state is approached was investigated (with a negative result) by Ren *et al.*[9] within the HFA. These authors also claimed[10] that the $\nu^*=\frac{1}{6}$ composite fermion state has lower energy than the corresponding bubble state in $N=2$ and that this liquid state could be an intermediate state between the Wigner crystal and the $M=2$ bubble state. (See, however, Ref. 8.) In any case, the difference in the cohesive energy of the various possible ground states at any given filling factor is usually quite small and the possibility that quantum fluctuations, disorder, finite extension of the wave function in the third dimension, screening corrections, etc., modify the above scenario cannot be ruled out.

The existence of the bubble state near filling factors $\nu^*\approx\frac{1}{4}$ and $\nu^*\approx\frac{3}{4}$ in $N=2$ was first shown by transport mea-

 

surements revealing its insulating behavior[2,3] and its nonlinear $I$-$V$ properties.[4] In more recent experiments, Lewis *et al.*[11] and Ye *et al.*[12] measured the diagonal conductivity $\sigma_{xx}$ of the 2DEG in the microwave regime and found sharp resonances in Re$[\sigma_{xx}]$ at some frequency. These resonances are strongest near $\nu^* \approx \frac{1}{4}$ and $\nu^* \approx \frac{3}{4}$ in level $N=2$. They appear for a range of partial filling factors around $\nu^* \approx \frac{1}{4}$ and $\nu^* \approx \frac{3}{4}$ and only for temperatures below 0.1 K. It is believed that these resonances are due to the excitation of the pinning mode of the bubble states realized at these filling factors. The experiments show no hint of discontinuous transitions among the different bubble states. It is possible that thermal or disorder effects may smear out any sharp effects on the pinning mode.

In light of these microwave experiments, it is natural to ask how one could observe a transition between bubble states, and also how one could distinguish between bubble states of different $M$ numbers. In this paper, we study how the behavior of several measurable physical properties of the bubble states evolve as the filling factor $\nu^*$ is increased from the Wigner crystal state at low filling to the stripe state at half-filling. We show that the series of transitions between bubble states lead to oscillations and discontinuities in the orbital magnetization and susceptibility. These effects are sizable so that the transitions between bubble states should be observable in a measurement of the magnetization or of the magnetic susceptibility. Such measurements have recently been performed on the 2DEG in the integer quantum Hall regime using an ultrasensitive torque magnetometer.[13] The sensitivity was sufficient to reveal the sawtooth pattern of oscillation of the magnetization, i.e., the de Haas–van Alphen effect, as well as the magnetization jumps occuring at odd filling factors from the occupation of different spin states of the same Landau level.

Our analysis also shows that the density of states has features that are directly related to the number of electrons per bubble. More precisely, we find that the number of low-energy subbands is equal to the number $M$ of electrons in the bubbles. If this density of state structure is not blurred by tunneling processes involving phonon excitations, then a double-well tunneling experiment or photoluminescence measurement could serve to determine $M$ and to follow the phase transitions between bubble states.

Working in the time-dependent Hartree-Fock approximation (TDHFA), we also compute the dispersion relation of the phonon as well as those of other higher-energy modes that correspond to excitations localized on the bubbles. These localized excitations are interesting because (in contrast to the phonon mode) they are gapped and probably less sensitive to the disordering potential. Their dispersion can be computed, in a first approximation, by neglecting disorder, which is difficult to take into account in these charge density wave states. We thus apply the TDHFA to show that the first-order transitions between the bubble states can be tracked by looking at the discontinuous behavior of the first few high-energy modes as a function of partial filling factor. In our analysis, we find that the frequency of the first excited energy modes are in a range accessible experimentally. Up to now, however, all conductivity measurements have concentrated on the pinning mode of either the stripe or bubble phases or, more recently, on the Wigner crystal phase near integer filling factor.[14]

The outline of the paper is as follows. In Sec. II, we briefly describe the Hartree-Fock procedure to compute the order parameters of the charge density wave states as well as the orbital magnetization and the one-particle density of states. We then introduce the time-dependent Hartree-Fock approximation and describe how we get the dispersion relation of the collective excitations in these ordered states. In Sec. III, we discuss our numerical results for these quantities. We conclude in Sec. IV, by discussing how our results could be related to the experiments of Lewis *et al.* and Ye *et al.*

## II. HARTREE-FOCK FORMALISM

### A. Order parameters

The bubble phase is a crystal state that can be described by the set of average values $\{\langle n(\mathbf{G})\rangle\}$, where $\langle n(\mathbf{G})\rangle$ is the ground-state average of the density operator and $\mathbf{G}$ is a reciprocal-lattice vector of the crystal. It is convenient, in the Landau gauge, to define a related density operator by the expression

$$\rho(\mathbf{G}) = \frac{1}{N_\varphi} \sum_X e^{-iG_x X + iG_x G_y l_\perp^2/2} c_{N,X}^\dagger c_{N,X-G_y l_\perp^2}, \qquad (1)$$

where $c_{N,X}^\dagger$ creates an electron in Landau level $N$ with guiding center quantum number $X$ and $N_\varphi$ is the Landau level degeneracy. This new density operator is related to the real density by the expression

$$n(\mathbf{G}) = N_\varphi F_{N,N}(\mathbf{G}) \rho(\mathbf{G}), \qquad (2)$$

where $F_{N,N}(\mathbf{G})$ is a form factor for the $N$th Landau level, which is given by

$$F_{N,N}(\mathbf{G}) = e^{-G^2\ell^2/4} L_N^0\left(\frac{G^2\ell^2}{2}\right), \qquad (3)$$

and $L_N^0(x)$ is a generalized Laguerre polynomial. At a semiclassical level, the average $\langle\rho(\mathbf{G})\rangle$ can be viewed as a Fourier transform of a ''guiding center density'' of cyclotron orbits.

In this paper, we make the usual approximations of neglecting any Landau level mixing and consider that the filled Landau levels are inert. It follows that the filled levels do not enter in our calculation and we will, whenever possible, drop the level index $N$ from now on to simplify the notation. Moreover, we assume that the partially filled level is completely spin polarized.

The average values $\langle\rho(\mathbf{G})\rangle$ are obtained by computing the single-particle Green's function

$$G(X,X',\tau) = -\langle T c_X(\tau) c_{X'}^\dagger(0)\rangle, \qquad (4)$$

whose Fourier transform we define as

$$G(\mathbf{G},\tau) = \frac{1}{N_\phi} \sum_{X,X'} e^{-(i/2)G_x(X+X')} \delta_{X,X'-G_y l_\perp^2} G(X,X',\tau), \qquad (5)$$

so that

$$\langle \rho(\mathbf{G}) \rangle = G(\mathbf{G}, \tau = 0^-). \tag{6}$$

We compute the single-particle Green's function of Eq. (5) by solving numerically the Hartree-Fock equation of motion

$$[i\omega_n + \mu] G(\mathbf{G}, i\omega_n) - \sum_{\mathbf{G}'} U(\mathbf{G}-\mathbf{G}') e^{i\mathbf{G}\times\mathbf{G}'\ell^2/2} G(\mathbf{G}', i\omega_n) = \delta_{\mathbf{G},0} \tag{7}$$

($\omega_n$ is a fermionic Matsubara frequency and we use the two-dimensional cross product as a short form for $\mathbf{q}\times\mathbf{G} \equiv q_x G_y - q_y G_x$), which follows from the mean-field Hamiltonian

$$H_{\mathrm{HF}} = N_\varphi \varepsilon_{N,\alpha} \rho(\mathbf{G}=0) + N_\varphi \sum_{\mathbf{G}} U_N(\mathbf{G}) \rho(\mathbf{G}), \tag{8}$$

where $\varepsilon_{N,\alpha} = (N+1/2)\omega_c - \alpha g^* \mu_B B/2$ is the noninteracting energy on an electron of spin $\alpha$ in Landau level $N$. The self-consistent Hartree-Fock potential $U(\mathbf{q})$ that appears in Eq. (7) is given by

$$U(\mathbf{q}) = [H_{N,N}(\mathbf{q}) - X_{N,N}(\mathbf{q})] \langle \rho(-\mathbf{q}) \rangle. \tag{9}$$

In Eq. (9), the Hartree-Fock interactions are given by

$$H_{N,N}(\mathbf{q}) = \left(\frac{e^2}{\kappa\ell}\right) \frac{1}{q\ell} e^{-q^2\ell^2/2} \left[ L_N^0\left(\frac{q^2\ell^2}{2}\right)\right]^2, \tag{10}$$

$$X_{N,N}(\mathbf{q}) = \left(\frac{e^2}{\kappa\ell}\right) \sqrt{2} \int_0^\infty dx\, e^{-x^2} [L_N^0(x^2)]^2 J_0(\sqrt{2} x q \ell), \tag{11}$$

where $\kappa$ is the dielectric constant of the host semiconductor and $J_0(x)$ is the Bessel function of order zero.

The electronic density in real space is obtained by the relation

$$\langle n(\mathbf{r}) \rangle = \frac{1}{2\pi\ell^2} \sum_{\mathbf{G}} e^{+i\mathbf{G}\cdot\mathbf{r}} F_{N,N}(\mathbf{G}) \langle \rho(\mathbf{G}) \rangle. \tag{12}$$

### B. Hartree-Fock energy

We solve the Hartree-Fock equation of motion [Eq. (7)] numerically by using an iterative approach that was described in detail in Refs. 15. Once the order parameters $\{\langle \rho(\mathbf{G}) \rangle\}$ are found, the Hartree-Fock energy per particle in the partially filled level can be written as

$$\frac{E_{\mathrm{HF}}}{N_s} = \frac{1}{2\nu^*} \sum_G [H_{N,N}(\mathbf{G})(1-\delta_{\mathbf{G},0}) - X_{N,N}(\mathbf{G})] |\langle \rho(\mathbf{G}) \rangle|^2, \tag{13}$$

where $\nu^*$ is the filling factor of Landau level $N$ and $N_s$ is the number of electrons in the partially filled level. The total filling factor of the two-dimensional electron gas is $\nu = 2N + \nu^*$.

### C. Density of states

In our iterative approach, the single-particle Green's function is computed by first finding the eigenvalues and eigenvectors of the interaction matrix

$$F_{\mathbf{G},\mathbf{G}'} \equiv U(\mathbf{G}-\mathbf{G}') e^{i\mathbf{G}\times\mathbf{G}'\ell^2/2}. \tag{14}$$

This matrix is Hermitian and can be diagonalized with the unitary transformation

$$F = V D V^\dagger,$$

where $V$ is the matrix of the eigenvectors of $F$ and $D_{i,j} = d_j \delta_{i,j}$ is the diagonal matrix of the eigenvalues of $F$. The Green's function is then readily given by

$$G(\mathbf{G}, \omega_n) = \sum_j \frac{V_{\mathbf{G},j} [V^\dagger]_{j,\mathbf{G}=\mathbf{0}}}{i\omega_n + (\mu - d_j)/\hbar}. \tag{15}$$

The density of states is defined as

$$g(\omega) = -\frac{1}{\pi} \int d\mathbf{r}\, \mathrm{Im}[G^R(\mathbf{r}, \mathbf{r}, \omega)], \tag{16}$$

where $G^R$ is the retarded single-particle Green's function, which can be computed from the eigenvalues and eigenvectors found above. We then have

$$g(\omega) = -\frac{N_\phi}{\pi} \mathrm{Im}\left[ \sum_j \frac{|V_{\mathbf{G}=\mathbf{0},j}|^2}{\omega + i\delta - d_j/\hbar}\right]. \tag{17}$$

### D. Collective modes

As shown in Refs. 15, the order parameters $\{\langle \rho(\mathbf{G}) \rangle\}$ can also be used to compute the density-density response function $\chi_{\mathbf{G},\mathbf{G}'}(\mathbf{k}, \tau)$ defined by

$$\chi_{\mathbf{G},\mathbf{G}'}(\mathbf{k}, \tau) = -N_\varphi \langle T \tilde{\rho}(\mathbf{k}+\mathbf{G}, \tau) \tilde{\rho}(-\mathbf{k}-\mathbf{G}', 0) \rangle, \tag{18}$$

where $\tilde{\rho} \equiv \rho - \langle \rho \rangle$. The collective modes of the bubble state are found from the poles of this response function. By following the poles with nonvanishing weight as the wave vector $\mathbf{k}$ is varied in the Brillouin zone of the reciprocal lattice, we get the dispersion relation of the phonon and higher-energy collective modes.

To find the equation of motion, in the TDHFA, for this two-particle Green's function, we first use the Hartree-Fock Hamiltonian of Eq. (8) to get the equation of motion for the Hartree-Fock approximation to $\chi_{\mathbf{G},\mathbf{G}'}(\mathbf{k}, \tau)$, which we call $\chi^0_{\mathbf{G},\mathbf{G}'}(\mathbf{k}, \tau)$. We obtain (neglecting, as usual, all Landau level as well as spin mixing)

$$i\Omega_n \chi^0_{\mathbf{G},\mathbf{G}'}(\mathbf{k}, \Omega_n) - 2i \sum_{\mathbf{G}''} \sin\left[\frac{(\mathbf{k}+\mathbf{G})\times(\mathbf{k}+\mathbf{G}'')\ell^2}{2}\right] \times U(\mathbf{G}''-\mathbf{G}) \chi^0_{\mathbf{G}'',\mathbf{G}'}(\mathbf{k}, \Omega_n) = -2i \sin\left[\frac{(\mathbf{k}+\mathbf{G})\times(\mathbf{k}+\mathbf{G}')\ell^2}{2}\right] \langle \rho(\mathbf{G}-\mathbf{G}') \rangle \tag{19}$$

($\Omega_n$ is a Matsubara bosonic frequency). The Hartree-Fock $\chi^0_{\mathbf{G},\mathbf{G}'}(\mathbf{k},\tau)$ corresponds to a single polarization bubble with Hartree-Fock propagators $G(\mathbf{G},\omega_n)$. The sum of the ladder diagrams involve the Fock (indirect) interaction $X_{N,N}(\mathbf{q})$ and is given by

$$\tilde{\chi}_{\mathbf{G},\mathbf{G}'}(\mathbf{k},\Omega_n)=\chi^0_{\mathbf{G},\mathbf{G}'}(\mathbf{k},\Omega_n)-\sum_{\mathbf{G}''}\chi^0_{\mathbf{G},\mathbf{G}''}(\mathbf{k},\Omega_n)\times X_{N,N}(\mathbf{k}+\mathbf{G}'')\tilde{\chi}_{\mathbf{G}'',\mathbf{G}'}(\mathbf{k},\Omega_n). \quad (20)$$

The two-particle Green's function $\tilde{\chi}_{\mathbf{G},\mathbf{G}'}(\mathbf{k},\Omega_n)$ contains only connected Feynman diagrams. The THDFA is achieved by summing the various bubble diagrams and is given by

$$\chi_{\mathbf{G},\mathbf{G}'}(\mathbf{k},\Omega_n)=\tilde{\chi}_{\mathbf{G},\mathbf{G}'}(\mathbf{k},\Omega_n)+\sum_{\mathbf{G}''}\tilde{\chi}_{\mathbf{G}'',\mathbf{G}'}(\mathbf{k},\Omega_n)\times H_{N,N}(\mathbf{k}+\mathbf{G}'')\chi_{\mathbf{G}'',\mathbf{G}'}(\mathbf{k},\Omega_n). \quad (21)$$

Equations (19)–(21) can easily be combined into a single equation that can be written, in obvious matrix form, as

$$\sum_{\mathbf{G}''}[i\Omega_n\delta_{\mathbf{G},\mathbf{G}'}-M_{\mathbf{G},\mathbf{G}''}(\mathbf{k})]\chi_{\mathbf{G}'',\mathbf{G}'}(\mathbf{k},i\Omega_n)=B_{\mathbf{G},\mathbf{G}'}(\mathbf{k}), \quad (22)$$

where the matrices $M_{\mathbf{G},\mathbf{G}}$ and $B_{\mathbf{G},\mathbf{G}'}$ are defined by

$$M_{\mathbf{G},\mathbf{G}'}(\mathbf{k})=-2i\left(\frac{e^2}{\hbar\kappa\ell}\right)\langle\rho(\mathbf{G}-\mathbf{G}')\rangle\sin\left[\frac{(\mathbf{G}\times\mathbf{G}')\ell^2}{2}\right]\times[H_{N,N}(\mathbf{G}-\mathbf{G}')-X_{N,N}(\mathbf{G}-\mathbf{G}')-H_{N,N}(\mathbf{G}')+X_{N,N}(\mathbf{G}')] \quad (23)$$

and

$$B_{\mathbf{G},\mathbf{G}'}(\mathbf{k})=2i\sin\left[\frac{(\mathbf{G}\times\mathbf{G}')\ell^2}{2}\right]\langle\rho(\mathbf{G}-\mathbf{G}')\rangle, \quad (24)$$

respectively. Because we have neglected all Landau level as well as spin mixing, the Green's function $\chi_{\mathbf{G},\mathbf{G}'}(\mathbf{k},\Omega_n)$ can only give information on intra-Landau-level excitations involving no spin flip. A more complete calculation of $\chi_{\mathbf{G},\mathbf{G}'}(\mathbf{k},\Omega_n)$ where inter-Landau-level and spin flip excitations are considered is detailed in the second paper of Ref. 16.

To solve for $\chi_{\mathbf{G},\mathbf{G}'}(\mathbf{k},i\Omega_n)$, we diagonalize the matrix $M_{\mathbf{G},\mathbf{G}''}(\mathbf{k})$ by the transformation

$$M=WTW^{-1}, \quad (25)$$

where $W$ is the matrix of the eigenvectors of $M$ and $T_{i,j}=t_j\delta_{i,j}$ is the diagonal matrix of its eigenvalues. The analytic continuation of $\chi_{\mathbf{G},\mathbf{G}'}(\mathbf{k},i\Omega_n)$ is given by

$$\chi_{\mathbf{G},\mathbf{G}'}(\mathbf{k},\omega)=\sum_{j,k}\frac{W_{\mathbf{G},j}(\mathbf{k})[W(\mathbf{k})^{-1}]_{j,k}B_{k,\mathbf{G}'}(\mathbf{k})}{\omega+i\delta-t_j(\mathbf{k})}. \quad (26)$$

The $j$th eigenvector in the matrix $W$ of the eigenvectors of the matrix $M$ gives the Fourier transform of the density modulation associated with the $j$th eigenvalue of $M$. We can thus produce an animation of the motion of the density modulation with the frequency $t_j$ and wave vector $\mathbf{k}$ by computing the time-dependent density

$$\delta n(\mathbf{r},t)\sim e^{-it_jt}\sum_{\mathbf{G}}e^{i(\mathbf{k}+\mathbf{G})\cdot\mathbf{r}}F_{N,N}(\mathbf{k}+\mathbf{G})W_{\mathbf{G},j}(\mathbf{k}) \quad (27)$$

at several values of $t$ in one period of the motion and then superimposing this density to the ground-state density given by the Hartree-Fock calculation [Eq. (12)]. We thus compute $n(\mathbf{r},t)=n_{\mathrm{HF}}(\mathbf{r})+\alpha\delta n(\mathbf{r},t)$ where $\alpha$ is choosen sufficiently small to satisfy $|\delta n(\mathbf{r},t)|<n_{\mathrm{HF}}(\mathbf{r})$.

### E. Orbital magnetization and magnetic susceptibility

The orbital magnetization and susceptibility can be obtained from the dependence of the Hartree-Fock energy with filling factor. At $T=0$ K, the orbital magnetization per electron is given by

$$m=-\frac{1}{N}\left(\frac{\partial E}{\partial B}\right), \quad (28)$$

while the orbital magnetic susceptibility per particle is

$$\chi=\left(\frac{\partial m}{\partial B}\right), \quad (29)$$

where $E$ is the ground-state energy of the 2DEG.

When all Landau levels are taken into account, the Hartree-Fock energy per particle, excluding the Zeeman contribution, is (for $0\leqslant\nu^*\leqslant 1$)

$$\frac{E^{\mathrm{total}}_{\mathrm{HF}}}{N_T}=\frac{1}{\nu}\sum_{M<N}\sum_{\alpha}(M+\tfrac{1}{2})\hbar\omega_c+\frac{\nu^*}{\nu}(N+\tfrac{1}{2})\hbar\omega_c-\frac{1}{2\nu}\left(\frac{e^2}{\kappa\ell}\right)\sum_{\alpha}\sum_{M<N}\sum_{M'<N}X_{M,M'}(\mathbf{G}=\mathbf{0})-\frac{1}{\nu}\left(\frac{e^2}{\kappa\ell}\right)\sum_{M<N}X_{M,N}(\mathbf{G}=\mathbf{0})\nu^*+\frac{1}{2\nu}\left(\frac{e^2}{\kappa\ell}\right)\sum_{\mathbf{G}}[H_{N,N}(\mathbf{G})(1-\delta_{\mathbf{G},0})-X_{N,N}(\mathbf{G})]|\langle\rho(\mathbf{G})\rangle|^2, \quad (30)$$

where

$$X_{N,M}(\mathbf{q})=\left(\frac{\min(M,N)!}{\max(M,N)!}\right)\int_0^{+\infty}dy\left(\frac{y^2}{2}\right)^{|N-M|}\times e^{-y^2/2}\left[L^{|N-M|}_{\min(N,M)}\left(\frac{y^2}{2}\right)\right]^2J_0(q\ell_\perp y) \quad (31)$$

is the exchange interaction between electrons in Landau levels $N$ and $M$, and $\alpha$ is the spin index. To derive this formula, we have assumed that all levels below $N$ are occupied and that only the spin level $\alpha=-1$ in Landau level $N$ is partially occupied. The *total* number of particles $N_T$ is assumed fixed.

With the definitions

$$\Lambda_0(N)=\sum_{M<N}(M+\tfrac{1}{2}), \tag{32}$$

$$\Lambda_1(N)=\sum_{M<N}\sum_{M'<N}X_{M,M'}(\mathbf{G}=\mathbf{0}), \tag{33}$$

$$\Lambda_2(N)=\sum_{M<N}X_{M,N}(\mathbf{G}=\mathbf{0}), \tag{34}$$

$$F(N,\nu^*)=\frac{1}{2\nu^*}\sum_{\mathbf{G}}[H_{N,N}(\mathbf{G})(1-\delta_{\mathbf{G},0}) -X_{N,N}(\mathbf{G})]|\langle\rho(\mathbf{G})\rangle|^2, \tag{35}$$

Eq. (30) can be written as

$$\frac{E_{\rm HF}^{\rm total}}{N_T}=2\Lambda_0(N)\frac{\hbar\omega_c}{\nu}+(N+\tfrac{1}{2})\frac{\nu^*}{\nu}\hbar\omega_c-\frac{1}{\nu}\left(\frac{e^2}{\kappa\ell}\right)\Lambda_1(N) -\frac{\nu^*}{\nu}\left(\frac{e^2}{\kappa\ell}\right)\Lambda_2(N)+\frac{\nu^*}{\nu}\left(\frac{e^2}{\kappa\ell}\right)F(\nu^*), \tag{36}$$

where

$$F(\nu^*)=\frac{1}{2\nu^*}\sum_{\mathbf{G}}[H_{N,N}(\mathbf{G})(1-\delta_{\mathbf{G},0})-X_{N,N}(\mathbf{G})]|\langle\rho(\mathbf{G})\rangle|^2, \tag{37}$$

is the (dimensionless) Hartree-Fock energy per particle in the partially filled level, i.e., the energy given in Eq. (13).

Differentiating Eq. (36) once (twice) with respect to the magnetic field at constant density and adding the spin contribution, we get the total magnetization (total spin susceptibility). We write

$$\mu=\mu_B\left(\frac{m}{m^*}\right)(\mu_1+\mu_2+\mu_3+\mu_4), \tag{38}$$

where $\mu_B=e\hbar/2mc$ is the Bohr magneton. The four contributions to the magnetization are defined (for $0\leqslant\nu^*\leqslant 1$) by

$$\mu_1=-8\Lambda_0\frac{1}{\nu}-2(N+\tfrac{1}{2})\left(1-\frac{4N}{\nu}\right),$$

$$\mu_2=\frac{1}{2}g^*\left(\frac{m^*}{m}\right)\left(1-\frac{4N}{\nu}\right),$$

$$\mu_3=\frac{3}{\sqrt{2}}r_s\Lambda_1(N)\frac{1}{\sqrt{\nu}}-\sqrt{2}r_s\Lambda_2(N)[-\tfrac{1}{2}\nu+3N]\frac{1}{\sqrt{\nu}},$$

$$\mu_4=\sqrt{2}r_s\sqrt{\nu}(\nu-2N)\frac{\partial F(\nu^*)}{\partial\nu^*} +\sqrt{2}r_s[-\tfrac{1}{2}\nu+3N]\frac{1}{\sqrt{\nu}}F(\nu^*). \tag{39}$$

Similarly, we write (for $0\leqslant\nu^*\leqslant 1$) the total magnetic susceptibility as the sum of the four contributions

$$\chi=\frac{e^2}{4\pi nm^*c^2}(\chi_1+\chi_2+\chi_3+\chi_4), \tag{40}$$

where

$$\chi_1=-8\Lambda_0(N)+8N(N+\tfrac{1}{2}),$$

$$\chi_2=-2Ng^*\left(\frac{m^*}{m}\right),$$

$$\chi_3=\frac{3r_s}{2\sqrt{2}}\Lambda_1(N)\sqrt{\nu}-\frac{1}{\sqrt{2}}r_s\Lambda_2(N)\left[\frac{\nu^{3/2}}{2}+3N\sqrt{\nu}\right],$$

$$\chi_4=\sqrt{2}r_s\left[\tfrac{1}{4}(\nu+6N)\sqrt{\nu}F(\nu^*)-(\nu+2N)\nu^{3/2}\frac{\partial F(\nu^*)}{\partial\nu^*} -(\nu-2N)\nu^{5/2}\frac{\partial^2F(\nu^*)}{\partial\nu^{*2}}\right]. \tag{41}$$

The four contributions to the magnetization and susceptibility come, respectively, from the kinetic energy $(\mu_1,\chi_1)$, the Zeeman energy $(\mu_2,\chi_2)$, the exchange energy between electrons in the filled levels or between electrons in the filled levels and those in level $N$ $(\mu_3,\chi_3)$, and the Hartree-Fock energy of electrons in level $N$ $(\mu_4,\chi_4)$. In Eq. (41), we have introduced the gas parameter $r_s=1/\sqrt{\pi na_B^2}$, where $a_B=\hbar^2\kappa/m^*e^2$ is the effective Bohr radius, and the effective $g$ factor $g^*$. We remark that our units for the susceptibility can also be written as $e^2/4\pi nm^*c^2=\mu_B^*/B_{\nu=1}$, where $\mu_B^*=e\hbar/2m^*c$ and $B_{\nu=1}$ is the magnetic field required to get a filling factor of $\nu=1$ for a total density of $n$.

## III. NUMERICAL RESULTS

We now discuss our numerical results for the physical quantities introduced above.

### A. Hartree-Fock energy

Figures 1(a)–1(c) shows the Hartree-Fock energy per electron as a function of filling factor for the bubble and stripe phases in Landau levels $N=2$, 3, and 5. The filling factors at which the transitions between states occur are indicated in an inset in each figure. In all cases, the transitions are of first order and the transition scenario is that described in the Introduction: the ground state evolves from the Wigner crystal at low filling, through a succession of bubble states with increasing values of guiding centers per bubble, and finally into the stripe state near half-filling. The number of possible bubble states increases with Landau level index $N$. Our results for $N=2$, 3 are in agreement with previously obtained Hartree-Fock energies for the bubble states.[8] Energies for $N=5$ have not been computed before. As shown in Ref. 8, the Hartree-Fock results are similar to those obtained by a DMRG calculation except that the region where the stripe phase is stable is wider in the DMRG calculation and, consequently, the bubble state with $N+1$ electrons per bubble disappears. Oscillations in the Laguerre polynomial entering the form factor in Eq. (3) make it difficult to com-

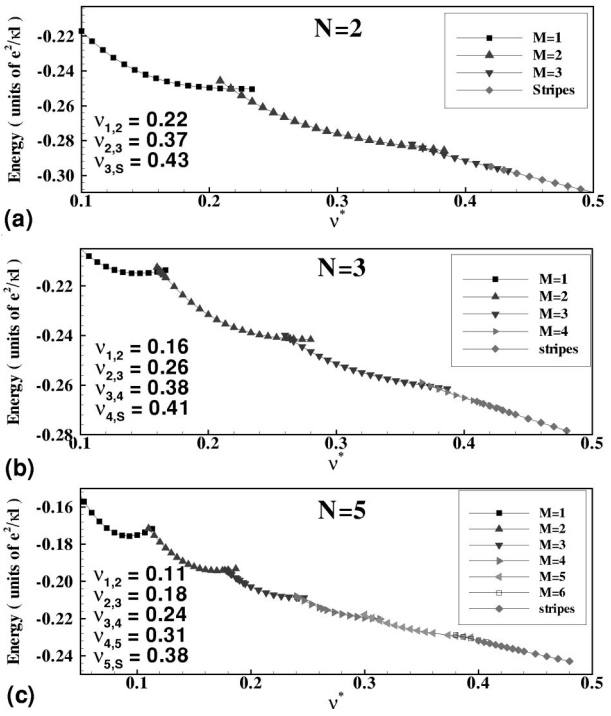


FIG. 1. Hartree-Fock energy per particle as a function of the filling factor $\nu^*$ of the partially filled level for the bubble and stripe phases in higher Landau level. The inset in each figure indicates the critical filling factor $\nu_{i,j}$ of the *partially* filled level at which the transition between bubble states or between the last bubble state and the stripe state occurs.

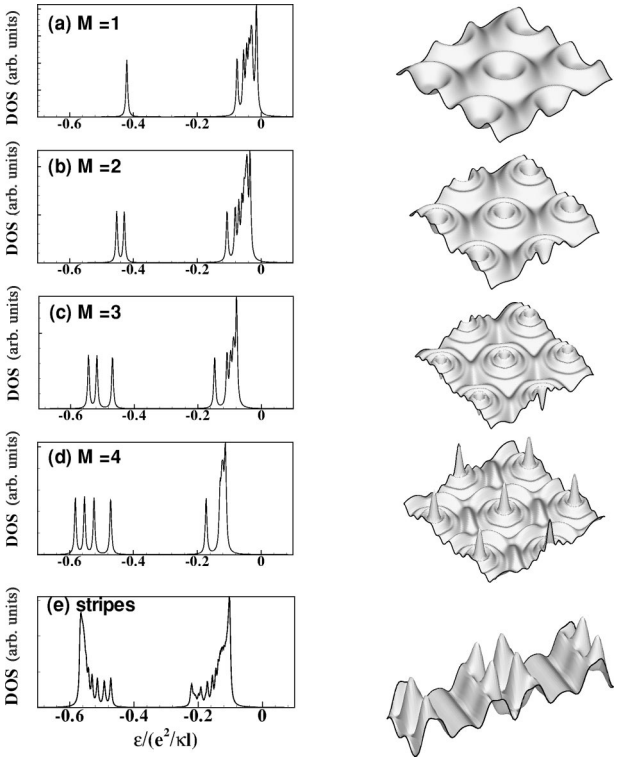


FIG. 2. Single-particle density of states and density pattern for bubble state with $M=1$, 2, 3, 4 electrons per bubble and for the stripe states in Landau level $N=3$. The filling factors are (a) $\nu^*=0.113$; (b) $\nu^*=0.173$; (c) $\nu^*=0.320$; (d) $\nu^*=0.406$; (e) $\nu^*=0.430$.

pute a numerically accurate phase diagram for higher Landau-level indices using our equation of motion technique.

### B. Density pattern

Figure 2 shows how the density pattern given by Eq. (12) evolves as the filling factor increases in Landau level $N=3$. When the bubbles are relatively far apart, the density pattern on each crystal site is well approximated by the trial wave function of Fogler and Koulakov.[6] For a bubble of $M$ electrons in Landau level $N$, that wave function is the Slater determinant

$$\Psi_N(\mathbf{r}_1,\mathbf{r}_2,\ldots,\mathbf{r}_M) = \begin{vmatrix} \varphi_{N,0}(\mathbf{r}_1) & \varphi_{N,0}(\mathbf{r}_1) & \cdots & \varphi_{N,0}(\mathbf{r}_M) \\ \varphi_{N,1}(\mathbf{r}_2) & \varphi_{N,1}(\mathbf{r}_2) & \cdots & \varphi_{N,1}(\mathbf{r}_M) \\ \vdots & \vdots & \vdots & \vdots \\ \varphi_{N,M}(\mathbf{r}_1) & \varphi_{N,M}(\mathbf{r}_2) & \cdots & \varphi_{N,M}(\mathbf{r}_M) \end{vmatrix}, \quad (42)$$

where

$$\varphi_{N,m}(\mathbf{r}) = C_{N,m}\left(\frac{r}{\ell}\right)^{|m-N|} e^{-r^2/4\ell^2} \times e^{i(N-m)\theta} L_{(N+m-|m-N|)/2}^{|m-N|}\left(\frac{r^2}{2\ell^2}\right)$$

is the normalized wave function of an electron in the symmetric gauge $\mathbf{A}=(-B_0y/2, B_0x/2, 0)$ with Landau level $N$ and angular momentum $m$. The one-particle density

$$n_N(\mathbf{r}) = \left[\prod_{i=2}^{i=M} \int d\mathbf{r}_i\right] |\Psi_N(\mathbf{r},\mathbf{r}_2,\ldots,\mathbf{r}_M)|^2 \quad (43)$$

is just

$$n_N(\mathbf{r}) = \sum_{m=1}^{m=M} |\varphi_{N,m}(\mathbf{r})|^2. \quad (44)$$

As the filling factor increases in the $M$th bubble state, the outer ring from each bubble gets closer to its neighbors and the density pattern given by Eq. (44) is strongly modified. When rings from two adjacent bubbles start to overlap, there is a transition to the $(M+1)$th bubble state. In Landau level $N$, the last bubble state before the transition to the stripe phase has $M=N+1$. We note that the stripe state obtained in our Hartree-Fock approximation is not the quantum Hall smectic state. It has density modulations along the stripes and can be described as a highly anisotropic Wigner crystal. However, it is likely that this state is unstable due to quantum fluctuations to the smectic state.[16]

### C. Density of states

Figure 2 shows the behavior of the single-particle density

of states $g(E)$ defined in Eq. (17) for Landau level $N=3$ and for filling factors corresponding to bubble states with $M=1$, 2, 3, and 4 electrons per bubble. In Landau level $N=0$ where the Wigner crystal state with $M=1$ is the ground state for all filling factors, our calculation for $g(E)$ reproduces the well-known Hofstadter butterfly structure. For $\nu^*=q/p$, the density of states consists of $p$ subbands of which $q$ low-energy bands are filled and separated by a gap from the remaining $p-q$ subbands. In Fig. 2, we see that the density of states in the bubble state has a different structure. The number of low-energy subbands that can be resolved by our numerical calculation clearly corresponds to the number $M$ of electrons per bubble. A measurement of the density of states, by a double-well tunneling experiment or photoluminescence, could serve to determine $M$. In computing the tunneling current, one would have to take into account other processes involved, particularly phonon shake-up. This is, however, beyond the scope of our paper and is left for future research. We note for now, however, that the typical phonon bandwidth (discussed below) is not larger than the splittings among the occupied bands in the density of states, so that the multiplicities of peaks associated with different bubble states are likely to survive such effects.

### D. Magnetic susceptibility

The Hartree-Fock energy shown in Fig. 1 has a discontinuous change of slope and curvature at the transitions between bubble states with different number $M$ of electrons per bubble. This, in turn, gives rise to discontinuities in the behavior of the magnetic susceptibility with filling factor. To show this, we compute the susceptibility in Landau level $N=3$ by numerically evaluating the first and second derivatives of the function $F(\nu^*)$ defined in Eq. (37). We use the parameters $\Lambda_0(3)=9/2$, $\Lambda_1(3)=6.29$, and $\Lambda_2(3)=1.32$ appropriate to $N=3$ and assume a typical total electronic density of $n=3\times10^{11}e/\mathrm{cm}^2$ so that the gas parameter is $r_s=1.011$. The other parameters are $g^*=0.45$ and the effective mass $m^*=0.067m$.

Figures 3(a) and 3(b) show the behavior of the four contributions to the magnetic moment and magnetic susceptibility defined in Eq. (39) and Eq. (41). The singular behavior (contributions $\mu_4$ and $\chi_4$) comes, in both cases, from the Coulomb interaction between electrons in the partially filled level. The magnetic moment and susceptibility change discontinuously at the transition between bubble states and between the bubble and the stripe state. In both cases the effect is sizable. Consequently, the transitions between bubble states should, in theory, be observable in a measurement of the magnetization or magnetic susceptibility.[13]

### E. Collective excitations

We now discuss the collective excitations of the bubble states. We compute the density-density response function of Eq. (26) and follow its poles when the wave vector **k** is varied along the edges of the irreducible Brillouin zone of the triangular lattice of the crystal. Figures 4(a)–4(f) show examples of the dispersion relation we obtain. In these figures, the dispersion is plotted along the path $\Gamma$-$J$-$X$-$\Gamma$, corresponding to the wave vectors $(k_x,k_y)=(0,0)$, $(2\pi/a)\times(1/\sqrt{3},1/3)$, $(2\pi/a)(1/\sqrt{3},0)$, $(0,0)$ where $a$ is the lattice constant. The wave vector $k$ represents the total distance, in reciprocal space and in units of $2\pi/a$ where $a$ is the lattice constant, along the path $\Gamma$-$J$-$X$-$\Gamma$ from the origin $\Gamma$. For a given value of **k**, Eq. (36) provides us with a way to image the motion of the density in a particular mode.

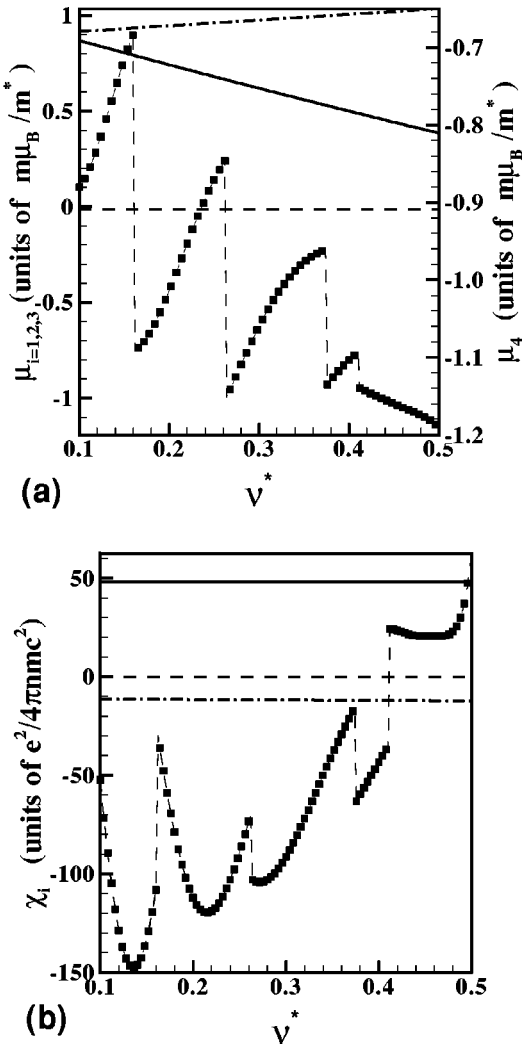


FIG. 3. (a) Change in the magnetic moment and (b) magnetic susceptibility with partial filling factor $\nu^*$ in Landau level $N=3$. The four contributions $i=1$ (solid), 2 (dashed), 3 (dashed dot), and 4 (squares) to $\mu$ or $\chi$ are defined in Eqs. (39) and (41).

We remark that our calculation does not include disorder so that the lowest-energy mode in Fig. 4 is a gapless phonon mode. For small wave vector, this phonon mode has the typical $\omega\sim k^{3/2}$ dispersion of a Wigner crystal. In the presence of disorder, this phonon mode would be gapped.

Upon entering a state with $M$ electrons per bubble, the dispersion and maximal frequency of the phonon mode first increases with the filling fraction. Near the critical filling factors $\nu^*_{M\to M+1}$ computed above in the HFA, the phonon mode starts to soften at a finite wave vector **k**. This indicates that the bubble states become locally unstable when the outer

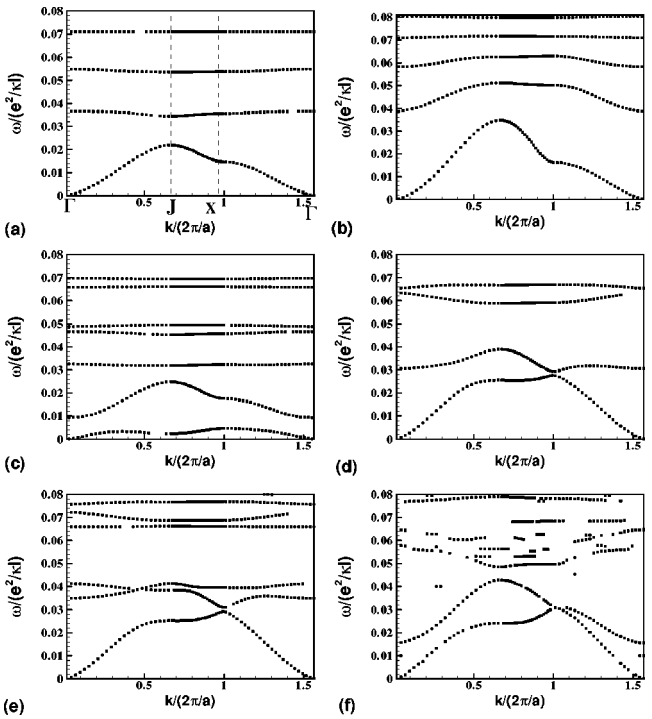


FIG. 4. Dispersion relations of the phonon and higher-energy modes in Landau level $N=3$ along the edges (path $\Gamma$-$J$-$X$-$\Gamma$) of the irreducible Brillouin zone of the triangular lattice. The filling factors and number of guiding centers per bubble are (a) $\nu^*=0.106$, $M=1$; (b) $\nu^*=0.161$, $M=1$; (c) $\nu^*=0.167$, $M=2$; (d) $\nu^*=0.206$, $M=2$; (e) $\nu^*=0.264$, $M=3$; (f) $\nu^*=0.380$, $M=4$.

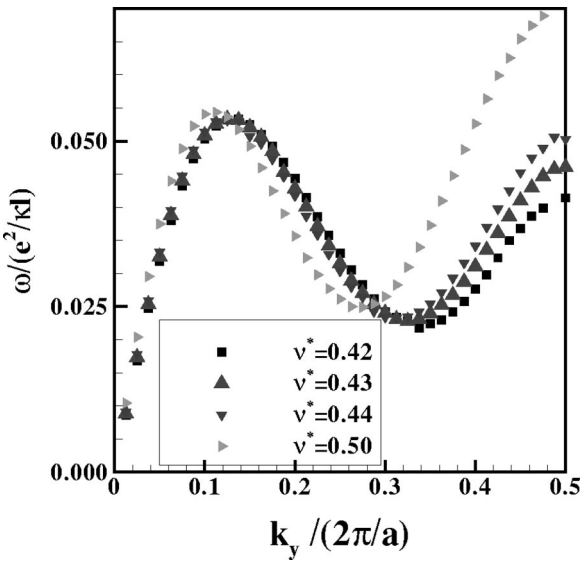


FIG. 5. Dispersion relation of the phonon mode of the modulated stripe state in Landau level $N=2$ for wave vector $\mathbf{k}$ along the direction of the stripes ($k_x=\pi/\xi$). Here, $a$ is the period of the modulations along the stripes and $\xi$ is the interstripe distance.

rings of adjacent bubbles start to touch. For the cases $N=2$, 3, 5 that we have studied, we find that the phonon mode frequency vanishes at this wave vector for $\nu^*>\nu^*_{M\to M+1}$ so that a second-order transition is preempted by a first-order one. This is also the case for the transition between the $M=N+1$ bubble state and the stripe state as we show in Fig. 5, where we plot the dispersion relation of phonon mode of the stripe state for wave vector $k$ along the direction of the stripes. The dispersion is shown for several values of the filling factor from $\nu^*=0.42$ to $\nu^*=0.50$ in Landau level $N=2$. It is clear that the dispersion of the phonon (and in particular the region around the roton minimum) does not change significantly near $\nu=0.428$, the filling factor at which the Hartree-Fock calculation predicts a transition between the $M=3$ bubble state and the stripe state.

For Landau-level index $N=1$, we find an interesting exception in that the softening of the phonon mode occurs for $\nu^*<\nu^*_{1\to 2}$. This indicates the possible existence of some new charge ordered state. We did not study this case further, however, since our approximations do not include correlations responsible for the correlated liquid states that are present in $N=1$.[8,17]

Another indication of the limitations of the HFA and TDHFA is that the last bubble state ($M=N+1$) is stable, in contrast to the DMRG result.[8] The DMRG method includes correlations neglected in the HFA and is, in principle, more exact than the HFA.[17] In any case, for values of $\nu$ where a bubble state is stable, we expect the TDHFA to give a reasonable approximation of the dispersion of its collective excitations.

We see from Fig. 4 that, above the phonon mode and in the region where the $M=1$ bubble state is stable, there is a series of higher-energy modes that are almost dispersionless except near filling factors where the transitions between bubble states do occur. As we explained in Ref. 15, more and more of these modes appear in the response function when we increase the size of the matrix $M_{\mathbf{G},\mathbf{G}}(\mathbf{k})$ in the equation of motion [Eq. (22)] for the response function $\chi_{\mathbf{G},\mathbf{G}'}(\mathbf{k},\omega)$. As more modes appear, the previous ones are not shifted in energy so that these modes are not numerical artifacts associated with the truncation of the infinite dimensional matrix $M_{\mathbf{G},\mathbf{G}}(\mathbf{k})$. For higher values of $M$, a general trend of the dispersion (except close to transition points) is that there are $M$ low-energy dispersive modes close in energy and a number of higher-energy much less dispersive modes. For large values of $M$, each bubble has a complex pattern of density modulations, and a large number of reciprocal lattice vectors are needed to describe its structure adequately. It follows that our numerical procedure is less precise in this case as can be seen from Fig. 4(f).

The small dispersion of the higher-energy modes suggests that they can be identified as local oscillations of the density within a bubble. This is indeed what can be seen from an animation of these modes using Eq. (36). Figure 6 shows several snapshots of these modes representing the motion of the density in the second, third, and fourth modes for $M=1$ in Landau level $N=2$. From these snapshots, we see that the higher-energy modes are density waves propagating along the rings of the bubbles. These modes can be readily identified by the number of wavelengths of these waves enclosed in the perimeter of the rings. For example, the second mode corresponds to the case where the perimeter of the

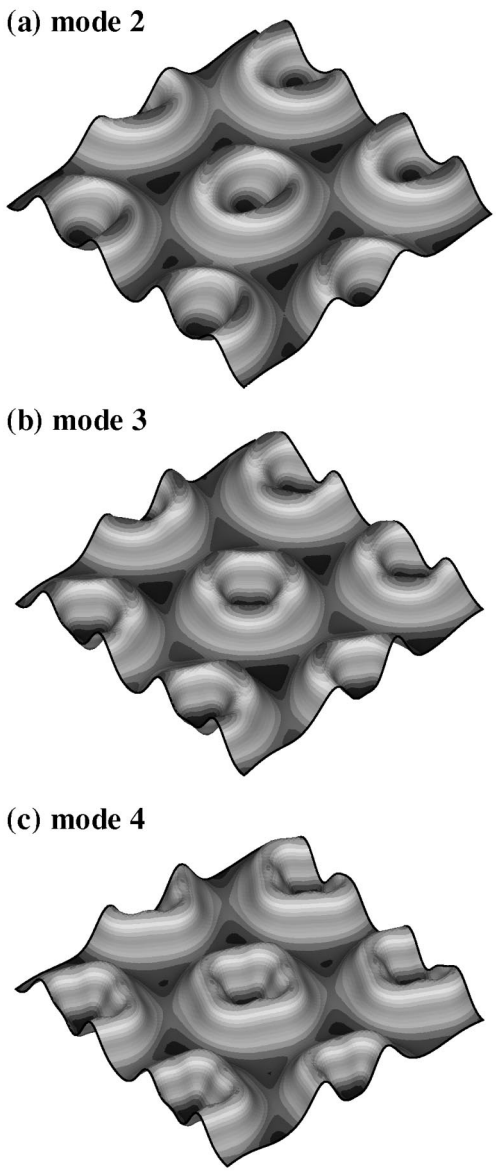


FIG. 6. Snapshots of the motion of the density in the second, third, and fourth higher-energy collective modes of the $M=1$ bubble state in Landau level $N=2$. The filling factor is $\nu^*=0.113$.

rings enclosed two wavelengths, the third mode to the case where the perimeter enclosed three wavelengths, and so on. When the separation between the bubbles decreases in a given $M$ bubble state, the density waves on each bubble become more and more coupled and the dispersion of the higher-energy modes can be very pronounced.

The frequency of the higher-energy collective modes change discontinuously with the transition between the bubble states. A measurement of the frequency of these modes could then provide yet another signature of the bubble states. It would be interesting if variations in the gap $\omega(\mathbf{k}\rightarrow\mathbf{0})$ of these higher-energy modes could be detected experimentally. Recently, Lewis *et al.*[11] reported the observation of an absorption peak in a measurement of the microwave absorption of a ultrahigh mobility two-dimensional electron

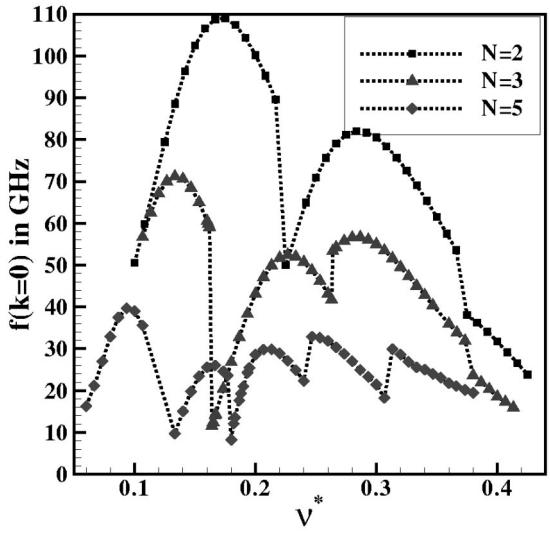


FIG. 7. Frequency $f(\mathbf{k}=\mathbf{0})$ of the first higher-energy collective mode of the bubble states versus filling factor $\nu^*$ in Landau levels $N=2$, 3, 5. We have assumed a density of $n=3.2\times10^{11}e/\mathrm{cm}^2$.

system in Landau levels $N=2$ and $N=3$. A peak of absorption occurs at a frequency that decreases as the center ($\nu^*=0.5$) of the Landau level is approached from either above or below. The resonances in the absorption are sharpest for filling factors $\nu^*$ around $\frac{1}{4}$ and $\frac{3}{4}$, corresponding to the values where the RIQHS occur in transport experiments.[2] At these filling factors, the resonance frequency is approximately $f=500$ MHz. It is natural to associate this resonance with a pinned phonon mode of the bubble states (of either electrons or holes for $\nu^*<0.5$ or $\nu^*>0.5$).

The higher-energy modes of the bubble states are gapped at $\omega(\mathbf{k}=\mathbf{0})=0$. In Fig. 7, we plot the gap $f(\mathbf{k}=\mathbf{0})=\omega(\mathbf{k}=\mathbf{0})/2\pi$ in the first high-energy mode as a function of filling factor $\nu^*$ for Landau levels $N=2$, 3, 5. To convert our frequencies (in units of $e^2/\hbar\kappa\ell$) into GHz, we assume $\kappa=12.9$ for the dielectric constant of the host semiconductor (GaAs) and take a typical density of $n=3.2\times10^{11}$ electrons/cm$^2$ so that $e^2/\hbar\kappa\ell=3827/\sqrt{\nu}$ GHz, where $\nu$ is the *total* filling factor of the 2DEG. At filling factor $\nu$, the magnetic field is given by $B=nh/e\nu=13.2/\nu$ T. As Fig. 7 shows, the transitions between bubble states lead to abrupt changes in the gap frequency when the filling factor is varied. The discontinuities are more pronounced for lower-Landau-level indices $N$. The frequency range of the first higher-energy mode is in a range of frequencies that can be obtained in a microwave absorption experiment; thus, such experiments can in principle probe the transitions among bubble states. We remark that other effects not included in our calculation, particularly the modeling of a finite width for the electronic wave function in the quantum well, could lead to a reduction of the gap frequency. This would make behavior such as that seen in Fig. 7 easier to detect.

To complete our calculation, it would be necessary to find out whether these higher-energy collective excitations are really detectable by a measurement of the absorption power. For this, one needs to compute the longitudinal conductivity $\sigma_{xx}$ in the presence of the disorder potential since otherwise

(by Kohn's theorem) only the cyclotron mode will show up in $\sigma_{xx}$. This calculation is beyond the scope of this paper but is in progress and will be reported elsewhere.

## IV. CONCLUSION

In this work, we have studied several physical properties of the bubble states that form in higher Landau levels. We have computed the energy and density pattern of the 2DEG ground state, in Landau levels $N=2$, 3, and 5, when the filling factor of the partially filled level is gradually increased from $\nu^*=0$ to $\nu^*=0.5$. In the Hartree-Fock approximation, the Wigner crystal at small $\nu^*$ evolves into the modulated stripe state near $\nu^*=0.5$ by passing through a succession of bubble states with increasing number of guiding centers per bubble. In all cases ($N>1$) that we have studied, the transitions are first order.

We have shown that several physical quantities such as the single-particle density of states, the magnetization, the magnetic susceptibility, and the dispersion of the collective excitations change discontinuously at the transition between these different ground states. We believe that these abrupt changes can be detected experimentally. In particular, we noticed that the density of states structure in the bubble states has features that allow one to determine, at least in principle, the number of guiding centers per bubble.

We have studied more closely the collective excitations of the bubble states and, in particular, the structure of the higher-energy modes (i.e., those modes above the phonon mode). In light of the recent microwave experiments by Lewis *et al.*,[11] we think that some of these modes are likely to be accessible experimentally. More work is needed to compute the real weight of these modes in the absorption. If these higher-energy modes can be detected in microwave absorption experiments, they will show a discontinuous change of the frequency. $f(\mathbf{k}=\mathbf{0})$ at each transition between the bubble states.

## ACKNOWLEDGMENTS

The authors thank R. Lewis and L. Engel for several useful discussions. This work was supported by a research grant (for R.C.) and undergraduate research grants (for C.D. and J.B.) from the Natural Sciences and Engineering Research Council of Canada (NSERC). H.A.F. acknowledges the support of the NSF through Grant No. DMR-0108451.

[1] A. A. Koulakov, M. M. Fogler, and B. I. Shklovskii, Phys. Rev. Lett. **76**, 499 (1996); M. M. Fogler, A. A. Koulakov, and B. I. Shklovskii, Phys. Rev. B **54**, 1853 (1996); R. Moessner and J. T. Chalker, *ibid.* **54**, 5006 (1996).

[2] M. P. Lilly, K. B. Cooper, J. P. Eisenstein, L. N. Pfeiffer, and K. W. West, Phys. Rev. Lett. **82**, 394 (1999).

[3] R. R. Du, D. C. Tsui, H. L. Stormer, L. N. Pfeiffer, K. W. Baldwin, and K. W. West, Solid State Commun. **109**, 389 (1999).

[4] K. B. Cooper, M. P. Lilly, J. P. Eisenstein, L. N. Pfeiffer, and K. W. West, Phys. Rev. B **60**, R11285 (1999).

[5] M. M. Fogler, in *High Magnetic Fields: Applications in Condensed Matter Physics and Spectroscopy* (Springer-Verlag, Berlin, 2002), pp. 98–138.

[6] M. M. Fogler and A. A. Koulakov, Phys. Rev. B **55**, 9326 (1997).

[7] E. H. Rezayi, F. D. M. Haldane, and K. Yang, Phys. Rev. Lett. **83**, 1219 (1999).

[8] N. Shibata and D. Yoshioka, Phys. Rev. Lett. **86**, 5755 (2001); D. Yoshioka and N. Shibata, Physica A **12**, 43 (2002).

[9] X. Ren, Shie-Jie Yang, Yue Yu, and Zhaobing Su, J. Phys.: Condens. Matter **14**, 3931 (2002).

[10] Shie-Jie Yang, Yue Yu, and Zhao-Bin Su, Phys. Rev. B **62**, 13557 (2000).

[11] R. M. Lewis, P. D. Ye, L. W. Engel, D. C. Tsui, L. N. Pfeiffer, and K. W. West, Phys. Rev. Lett. **89**, 136804 (2002).

[12] P. D. Ye, L. W. Engel, D. C. Tsui, R. M. Lewis, L. N. Pfeiffer, and K. West, Phys. Rev. Lett. **89**, 176802 (2002).

[13] S. A. J. Wiegers, M. Specht, L. P. Lévy, M. Y. Simmons, D. A. Ritchie, A. Cavanna, B. Etienne, G. Martinez, and P. Wyder, Phys. Rev. Lett. **79**, 3238 (1997).

[14] Yong Chen, R. M. Lewis, L. W. Engel, D. C. Tsui, P. D. Ye, L. N. Pfeiffer, and K. W. West, Phys. Rev. Lett. **91**, 016801 (2003); R. M. Lewis, Yong Chen, L. W. Engel, D. C. Tsui, P. D. Ye, L. N. Pfeiffer, and K. W. West, cond-mat/0307182 (unpublished).

[15] R. Côté and A. H. MacDonald, Phys. Rev. Lett. **65**, 2662 (1990); Phys. Rev. B **44**, 8759 (1991).

[16] H. A. Fertig, Phys. Rev. Lett. **82**, 3693 (1999); R. Côté and H. A. Fertig, Phys. Rev. B **62**, 1993 (2000); Hangmo Yi, H. A. Fertig, and R. Côté, Phys. Rev. Lett. **85**, 4156 (2000).

[17] A recent study by N. Shibata and D. Yoshioka, [Phys. Rev. Lett. **86**, 5755 (2003)] using the DMRG method shows that the $N=1$ level supports Wigner crystal, FHQE, stripes, and pairing states.